THE JOURNAL OF PHYSICAL CHEMISTRY Letters

Letter

Cite This: J. Phys. Chem. Lett. 2018, 9, 3766−3771

pubs.acs.org/JPCL

Theory for Nonlinear Spectroscopy of Vibrational Polaritons

Raphael F. Ribeiro,[†] Adam D. Dunkelberger,[‡] Bo Xiang,[§] Wei Xiong,[†,§] Blake S. Simpkins,[‡] Jeffrey C. Owrutsky,[‡] and Joel Yuen-Zhou*[,†]

[†]Department of Chemistry and Biochemistry, University of California, San Diego, La Jolla, California 92093, United States

[‡]Chemistry Division, Naval Research Laboratory, Washington, District of Columbia 20375, United States

[§]Materials Science and Engineering Program, University of California, San Diego, La Jolla, California 92093, United States

Supporting Information

ABSTRACT: Molecular polaritons have gained considerable attention due to their potential to control nanoscale molecular processes by harnessing electromagnetic coherence. Although recent experiments with liquid-phase vibrational polaritons have shown great promise for exploiting these effects, significant challenges remain in interpreting their spectroscopic signatures. We develop a quantum-mechanical theory of pump−probe spectroscopy for this class of polaritons based on the quantum Langevin equation and the input−output theory. Comparison with recent experimental data shows good agreement upon consideration of the various vibrational anharmonicities that modulate the signals. Finally, a simple and intuitive interpretation of the data based on an effective mode-coupling theory is provided. Our work provides a solid theoretical framework to elucidate nonlinear optical properties of molecular polaritons as well as to analyze further multidimensional spectroscopy experiments on these systems.

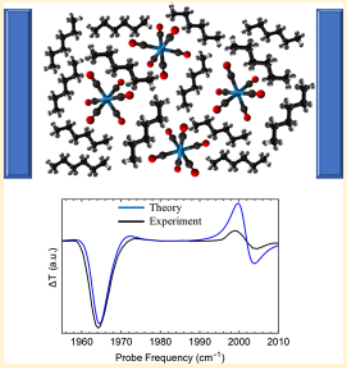

The strong coupling regime between optical microcavities and molecular vibrational modes has been recently achieved with polymers,[1−4] proteins,[5] liquid-phase solutions,[6−9] and neat liquids.[10] These works have unambiguously shown the existence of a novel class of hybrid optical excitations (vibrational polaritons) consisting of superpositions of delocalized molecular vibrations and microcavity electromagnetic (EM) field modes.[11] Given that polariton properties are tunable, the strong coupling of light and vibrational degrees of freedom opens up new routes for the control of chemical processes.[11,12]

Vibrational polaritons can be detected whenever a microcavity mode and the collective[13−15] vibrational polarization exchange energy at a rate that is faster than their dephasing.[11] Notably, in disordered media such as liquid-phase solutions, the (bare) vibrational modes are effectively dispersionless and may be assumed to be localized and uncorrelated. Thus a significant feature of the strong coupling regime is the introduction of a mesoscopic coherence length on the hybrid material infrared (IR) polarization.[16−18] This key point makes polaritons substantially different from conventional molecular states. Similar is true in the case of disordered organic excitons in molecular aggregates: Their excitations are at most delocalized about not more than a few hundreds of chromophores[19,20] due to dipolar interactions, but, upon strong coupling, a coherence length on the order of micrometers for polariton states is observed.[16,17] In fact, the field of organic semiconductor cavity polaritons has witnessed a surge in the last 15 years, with a variety of exciting phenomena demonstrated experimentally[21−27] and interesting theoretical predictions awaiting observation.[28−35] However, despite the similarity in the linear response of electronic and vibrational polaritons, there exist obvious differences in their nonlinear dynamics. In particular, vibrational modes can be well-approximated at low energies by weakly perturbed harmonic oscillators, whereas the same is generically not true for the electronic degrees of freedom. Thus intriguing phenomena have been recently observed under liquid-phase vibrational strong-coupling without clear counterpart in exciton−polariton systems. This includes, for example, the suppression and potential change of mechanism of an electronic ground-state chemical reaction,[6] and, among other features, the significant derivative line-shape and wave-vector dependence of vibrational polariton dynamics in the cavity−$W(CO)_6$ pump−probe (PP) spectra first reported by Dunkelberger et al.[9,36] Nonlinear spectroscopy is a particularly important tool to uncover the fundamental properties of vibrational polaritons[37] because it directly probes excited-state dynamics and thus the vibrational anharmonicity without which chemical reactions would not occur. Motivated by the intriguing PP spectra of vibrational polaritons first reported in ref 9 and the recent 2D spectra of Xiang et al.,[38] we present in this Letter a quantum-mechanical (QM) model for vibrational polariton PP spectroscopy including the effects of both mechanical and electrical anharmonicity of molecular modes.

Theory of PP Response of Vibrational Polaritons. We consider a setup with N identical independent vibrational (molecular) degrees of freedom strongly coupled to a single-mode planar Fabry−Perot (FP) microcavity[39] (Figure 1). The former are

Received: April 15, 2018
Accepted: May 31, 2018
Published: May 31, 2018

DOI: 10.1021/acs.jpclett.8b01176
J. Phys. Chem. Lett. 2018, 9, 3766−3771

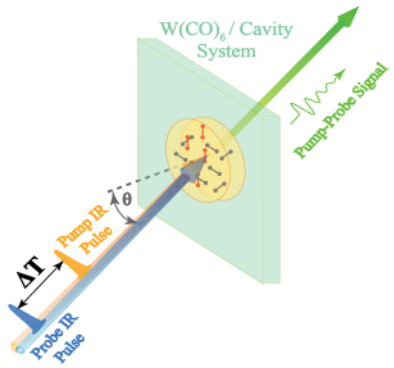

Figure 1. Experimental setup for pump−probe spectroscopy of polaritons formed from $W(CO)_6$ molecules embedded in an optical microcavity

assumed to be weakly coupled to intramolecular modes and solvent degrees of freedom (bath), whereas the latter is weakly coupled to the external (vacuum) EM modes on the left- and right-hand sides of its transverse direction. Thus the total Hamiltonian is given by a sum of three contributions $H = H_c + H_m + H_{mc}$, where H_c and H_m are the Hamiltonians describing the bare cavity and vibrational dynamics weakly coupled to their corresponding baths, whereas H_{mc} denotes the cavity−matter interaction (see SI Sec. I.). Alternatively, $H = H_0 + H_{anh}$, where H_0 generates the hybrid system linear dynamics and is given by

$$H_0 = \hbar\omega_0 \sum_{i=1}^{N} a_i^\dagger a_i + \hbar\omega_c b^\dagger b + \hbar g_1 \sum_{i=1}^{N} (a_i^\dagger b + b^\dagger a_i) + H_{SB} \tag{1}$$

where $\omega_0(\omega_c)$ is the molecular (cavity mode) fundamental frequency, a_i (b) is the ith molecule (cavity mode) annihilation operator, $\hbar g_1$ is the (real) single-molecule light-matter coupling, and H_{SB} contains the free dynamics of the molecular bath and external EM field along with their bilinear couplings to the molecular vibrations, and optical cavity, respectively (the explicit expressions are given in the SI Sec. I). The nonlinear dynamics of the system is generated by

$$H_{anh} = -\hbar \sum_{i=1}^{N} [\Delta a_i^\dagger a_i^\dagger a_i a_i - g_3(b^\dagger a_i^\dagger a_i a_i + a_i^\dagger a_i^\dagger a_i b)] \tag{2}$$

where the bare anharmonic shift Δ is >0 because the $1 \rightarrow 2$ vibrational transition has a lower frequency than ω_0 by 2Δ; that is, $\omega_{12} = \omega_0 - 2\Delta$, whereas g_3 can be either positive or negative as it represents the deviation of the vibrational $1 \rightarrow 2$ transition dipole moment (μ_{12}) from the corresponding result for the harmonic oscillator. In particular, g_3 manifests itself by the relation $\mu_{12} = \sqrt{2}\mu_{01}(1 + g_3/g_1)$[40,41] so that if g_3 and g_1 have the same (opposite) sign, then the μ_{12} of the anharmonic system will be larger (smaller) relative to that of a harmonic. Because Δ parametrizes the anharmonicity of molecular motion, its effect is called mechanical (nuclear) anharmonicity. The other term in eq 2 is known as electrical anharmonicity,[41−43] as it represents a deviation from harmonic behavior in the interaction between the molecules and the electric field of light. Note that for the purposes of describing the PP spectra of refs 9 and 38, the only relevant molecular transitions are $0 \rightarrow 1$ and $1 \rightarrow 2$. In particular, while the observed bare molecule PP spectra showed excited-state absorption peaks due to $2 \rightarrow 3$ and $3 \rightarrow 4$ transitions, no PP signal was observed near the corresponding frequencies in the experiments under the strong coupling regime. The reason is that the transitions other than $0 \rightarrow 1$ and $1 \rightarrow 2$ are highly off-resonant with the cavity. This also motivates the choice of anharmonicity parameters in eq 2.

We employ input−output theory[44−47] to estimate the PP transmission spectrum of vibrational polaritons. The strategy of the input−output method is to relate the microcavity EM field at a time t with the state of the external EM field at earlier and later times $t_i < t$ and $t_f > t$, respectively. The early and late external EM fields are denoted input and output fields, respectively (see SI Sec. I.A.). In the SI Sec. I, we show that the cavity mode annihilation operator satisfies the following Heisenberg−Langevin equation of motion

$$\frac{d}{dt}b(t) = -i\left(\omega_c - i\frac{\kappa}{2}\right)b(t) - \sqrt{\frac{\kappa}{2}}\,b_{in}^{L}(t) - ig_1P_1(t) - ig_3P_3(t) \tag{3}$$

where $\kappa/2$ is the cavity line width, $P_1(t)$ and $P_3(t)$ are molecular polarization operators to be described below, and $b_{in}^{L}(t)$ is the left input EM field operator (see SI Sec. I.A). In particular, for the system studied here, $b_{in}^{L}(t)$ represents the driving of the hybrid cavity at time t by an external EM field prepared at an earlier time $t_i < t$. As demonstrated in the SI (Sec. I.A.), there exists a result analogous to eq 3 for the cavity operator $b(t)$ in terms of left and right output operators $b_{out}^{L}(t)$ and $b_{out}^{R}(t)$, respectively. These operators encode the state of the external EM field in each of the external spatial regions at future times $t_f > t$ (see, e.g., SI eqs S8 and S12). The following (input−output) relation (proved in the SI Sec. I.A)[44] between input and output EM field operators is essential for the direct comparison of theory predictions and experimental observations

$$b_{out}^{L}(t) - b_{in}^{L}(t) = \sqrt{\frac{\kappa}{2}}\,b(t) = b_{out}^{R}(t) - b_{in}^{R}(t) \tag{4}$$

This allows us to obtain the output EM fields given the microcavity response and the input field. In particular, for the assumed geometry the (normalized) transmission $T(\omega)$ and reflection $R(\omega)$ spectra of the system are given by the following ratio of external EM field spectral densities

$$T(\omega) = \frac{|\langle b_{out}^{R}(\omega)\rangle|^2}{|\langle b_{in}^{L}(\omega)\rangle|^2} \tag{5}$$

$$R(\omega) = \frac{|\langle b_{out}^{L}(\omega)\rangle|^2}{|\langle b_{in}^{L}(\omega)\rangle|^2} \tag{6}$$

From eq 4, it follows that with $b_{in}^{R}(t) = 0$, $T(\omega)$ can be obtained in terms of the cavity polarization via the Fourier transform (FT) of the identity

$$b_{out}^{R}(t) = \sqrt{\frac{\kappa}{2}}\,b(t) \tag{7}$$

Hence, to obtain the transmission spectrum, we need to solve eq 3, which is coupled to Heisenberg−Langevin equations of motion for the molecular polarization operators $P_1(t) = \sum_i a_i(t)$ and $P_3(t) = \sum_i (a_i^\dagger a_i a_i)(t)$ given by

DOI: 10.1021/acs.jpclett.8b01176
J. Phys. Chem. Lett. 2018, 9, 3766−3771

$$\frac{dP_1(t)}{dt} = -i\omega_0 P_1(t) - \frac{\gamma_m}{2}P_1(t) + 2i\Delta P_3(t) - ig_1 Nb(t) - 2ig_3 \sum_{i=1}^{N} (a_i^\dagger a_i b)(t) - ig_3 b^\dagger(t) \sum_{i=1}^{N} (a_i a_i)(t) \quad (8)$$

$$\frac{dP_3(t)}{dt} = -i(\omega_0 - 2\Delta)P_3(t) - \frac{3\gamma_m}{2}P_3(t) - 2i(g_1 + g_3) \sum_{i=1}^{N} (a_i^\dagger a_i b)(t) - 3ig_3 \sum_{i=1}^{N} (a_i^\dagger a_i^\dagger a_i a_i b)(t) + ig_1 b^\dagger(t) \sum_{i=1}^{N} (a_i a_i)(t) - 2\Delta \sum_{i=1}^{N} (a_i^\dagger a_i^\dagger a_i a_i a_i)(t) \quad (9)$$

where $\gamma_m > 0$ is the full width at half-maximum of the molecular vibrations induced by interaction with a local bath (see SI Sec. I.B).

In this Letter, we focus on the pump-induced probe transmission observed at sufficiently long waiting (PP delay) time T,[37,48] such that coherences have dephased and thus only transient molecular population variables need to be retained for an accurate description of the optical response. In other words, we assume the only significant effect of the pump on the system at the probe delay time is the generation of a transient molecular excited-state population inside the cavity. We also neglect any photonic population at the PP time delay. This assumption is consistent with the fact that in the experiments that we ultimately compare our theory to the cavity photon lifetime and probe delay are approximately 5 and 25 ps, respectively.[9,38] Thus the last two terms of eq 9 can be neglected, as their averages tend to zero at the PP time T. We also assume that the expectation value $\langle a_i^\dagger a_i^\dagger a_i a_i\rangle(t)$ is much smaller than $\langle a_i^\dagger a_i\rangle(t)$ for $t \approx T$. This is reasonable, as we expect that after pumping the system with a classical field each factor of $a_i(t)$ contributes roughly a factor of $\approx\sim e_m^{-\gamma t/2}$ to these expectation values. In view of the listed conditions, we only need a single parameter $f^{pu} = \sum_{i=1}^{N}\langle a_i^\dagger a_i\rangle(T)/N$ to represent the pump-induced nonequilibrium state of the system at the time where the probe acts. In this case, $\langle P_3\rangle(t)$ can be quickly obtained as a function of f^{pu} via

$$\frac{d\langle P_3\rangle}{dt} = -i(\omega_{12} - i\gamma_3)\langle P_3\rangle(t) - 2i(g_1 + g_3)Nf^{pu}\langle b\rangle(t) \quad (10)$$

$$\langle P_3\rangle(\omega') = Nf^{pu}A_3(\omega')\langle b\rangle(\omega') \quad (11)$$

where $\langle b\rangle(t)[\langle b\rangle(\omega')]$ is the expectation value of (the FT of) the Heisenberg operator $b(t)$, $\gamma_3 = 3\gamma_m/2$, and $A_3(\omega') = 2(g_1 + g_3)/[\omega' - \omega_{12} + i\gamma_3]$. Similarly, we obtain the following approximation for $\langle P_1\rangle(\omega')$

$$\langle P_1\rangle(\omega') = NA_1(\omega', f^{pu})\langle b\rangle(\omega') \quad (12)$$

where

$$A_1(\omega', f^{pu}) = \frac{g_1 + 2g_3 f^{pu} - 2\Delta f^{pu}A_3(\omega')}{\omega' - \omega_0 + i\gamma_1}\langle b\rangle(\omega') \quad (13)$$

and $\gamma_1 = \gamma_m/2$. Note that if $f^{pu} = 0$, then $A_1(\omega',0) = g_1/(\omega' - \omega_0 + i\gamma_1)$, which is the appropriate result in the absence of a pump-induced excited-state population. The presented solutions for the matter polarization equations of motion can now be introduced to the frequency-domain representation of eq 3. Its solution can be directly inserted in eq 7 to generate $b_{out}^R(\omega)$ in terms of the (FT of the) input-probe field $b_{in}^L(\omega)$

$$\langle b_{out}^R\rangle(\omega') = [-i\frac{\kappa}{2}(\omega' - \omega_0 + i\gamma_1)(\omega' - \omega_{12} + i\gamma_3)]/[(\omega' - \omega_c + i\kappa/2)(\omega' - \omega_0 + i\gamma_1)(\omega' - \omega_{12} + i\gamma_3) - NA(\omega', f^{pu})]\langle b_{in}^L\rangle(\omega') \quad (14)$$

where

$$A(\omega', f^{pu}) = g_1^2[\omega' - (\omega_0 - 2\Delta) + 3i\gamma_m/2] + f^{pu}B(\omega') \quad (15)$$

$$B(\omega') = g_3[2(2g_1 + g_3)(\omega' - \omega_0) + (4g_1 + g_3)i\gamma_m] - 4\Delta g_1^2 \quad (16)$$

Equation 14 is the main result of this work. It can be applied to eq 5 to express the transmission spectrum of a cavity strongly coupled to vibrational modes, given a pump-induced vibrational excited-state population (Nf^{pu}). Note that if $g_3 = \Delta = 0$, then no nonlinear signal exists, consistent with the fact that harmonic systems do not exhibit a nonlinear response.[49]

Comparison to Experimental Results. We compare the predictions of our model with experiments that utilized solutions of $W(CO)_6$ in hexane.[9,38] In these, the triply degenerate carbonyl asymmetric stretch T_{1u} of the molecule was chosen to be strongly coupled to a resonant IR FP cavity. The following parameters were taken from the experiments of Xiang et al.,[38] $\omega_c = \omega_0 = 1983\ cm^{-1}$, $\gamma_m = 3\ cm^{-1}$, $\kappa = 11\ cm^{-1}$, $\Delta = 7.5\ cm^{-1}$, and $g_1\sqrt{N} = 19\ cm^{-1}$. Because the electrical anharmonicity constant is unknown for this mode, we chose $g_3/g_1 = -0.25$, as a similar value was reported by Khalil et al.[41] for the carbonyl stretch in a different system (although with almost equal anharmonic shift to the referred mode). Additionally, we take $f^{pu} = 0.075$ in all reported results. (For a discussion of absorption that validates this estimate, see SI Sec. I.D.) In Figure 2, experimental and theoretical results are compared for

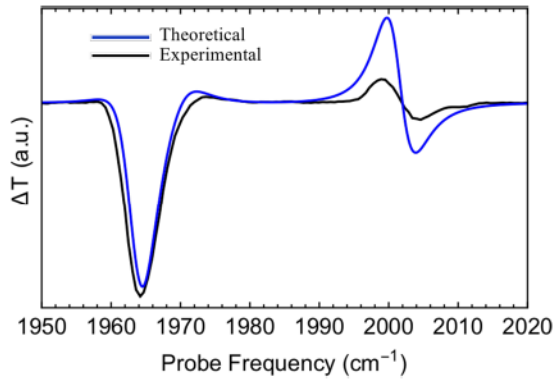

Figure 2. 25 ps experimental (black)[38] and theoretical (blue) PP spectrum obtained assuming $f^{pu} = 0.075$ and $\omega_c = \omega_0 = 1983\ cm^{-1}$.

the polariton PP (differential transmission) spectrum $\Delta T(\omega) = T^{pu}(\omega) - T^0(\omega)$, where $T^{pu}(\omega)$ is the transmission spectrum after excitation of the system with the pump and $T^0(\omega)$ is the linear transmission obtained in the absence of pumping. The experimental spectrum[38] was obtained after a probe delay time of 25 ps. (See also ref 9.) The two dominant features of the experimental PP spectrum are reproduced by our theory: the large negative signal in a neighborhood of the linear LP

DOI: 10.1021/acs.jpclett.8b01176
J. Phys. Chem. Lett. 2018, 9, 3766−3771

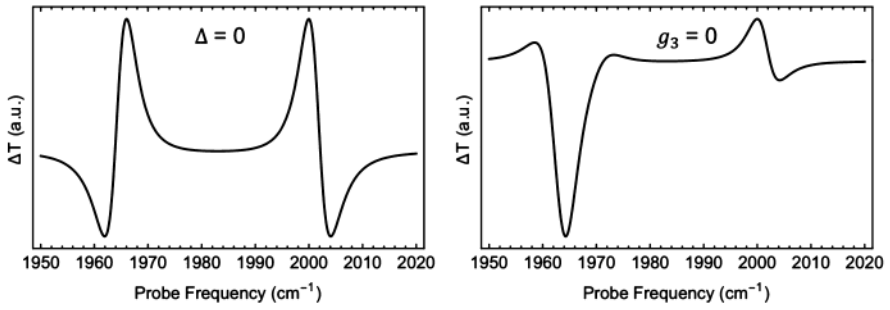

Figure 3. Theoretical PP spectrum with vanishing mechanical (left) or electrical anharmonicity (right).

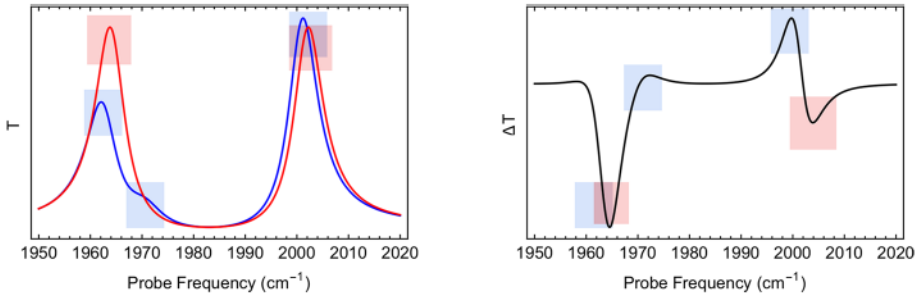

Figure 4. Left: Theoretical transmission spectrum in the presence (blue) and absence of pumping (red). Right: Theoretical PP spectrum (difference between blue and red curves of left) with identified resonances.

frequency and the red shift of the UP resonance. The theoretical prediction for the intensity of the latter is overestimated compared with the experimental result. This can be attributed to the various approximations employed in the derivation of eq 14. To understand the effects of vibrational anharmonicity on the polariton spectrum, we show in Figure 3 the theoretical PP spectrum obtained when either electrical (right) or mechanical anharmonicity (left) is turned off. In this system, electrical anharmonicity gives rise to a transient spectrum with blue (red) shift for the LP (UP) in conformity with the notion that it reduces the effective light−matter interaction (compared with a harmonic model). However, for systems with $\mu_{1\to 2} > \sqrt{2}\mu_{0\to 1}$, the Rabi splitting would be increased. Note that the transmission peaks of LP and UP remain symmetrically distributed around the fundamental frequency. Mechanical anharmonicity also has simple effects on the polariton PP spectrum (Figure 3, right): The UP shows a mild red shift, and the LP resonance splits into two. Note that while the theoretical spectrum with $g_3 = 0$ resembles the experimental in Figure 1, the former contains a positive bump near 1960 cm^{-1} which is absent from the latter. Thus the best agreement with experiment is observed when both electrical and nuclear anharmonicities are included in the theoretical model. To provide a simple physical picture of the vibrational-polariton PP spectra, we note that when $\gamma_m \to 0$ (for the case with significant molecular damping, see SI Sec. II), the resonances of the pump-induced transmission (eq 14) can be obtained as eigenvalues of the mode-coupling matrix

$$h(f^{pu}) = \begin{pmatrix} \omega_c - i\kappa/2 & g_1\sqrt{N}\sqrt{1-2f^{pu}} & g_2\sqrt{2f^{pu}N} \\ g_1\sqrt{N}\sqrt{1-2f^{pu}} & \omega_{01} & 0 \\ g_2\sqrt{2f^{pu}N} & 0 & \omega_{12} \end{pmatrix} \quad (17)$$

where $g_2 = g_1 + g_3$. The elements $[h(f^{pu})]_{ij}$ with $i = j$ correspond to the bare cavity photon and matter excitation frequencies, while the off-diagonal entries contain the effective coupling between matter polarization and the cavity mode. Thus we may assign the matrix index $i = 1$ to the cavity photon, whereas $i = 2$ and $i = 3$ correspond to the matter polarization components $P_{0\leftrightarrow 1}$ and $P_{1\to 2}$. Physically, $P_{0\leftrightarrow 1}$ represents the effective material polarization due to stimulated emission and ground-state bleach, and $P_{1\to 2}$ is the excited-state absorption contribution. Hence, the off-diagonal elements of $h(f^{pu})$ can be interpreted as couplings between the cavity and the different components of matter polarization. Note the interaction between $P_{1\to 2}$ and the cavity photon depends linearly on $\sqrt{f^{pu}N}$, while that between $P_{0\leftrightarrow 1}$ and the cavity depends on $\sqrt{(1-f^{pu})N - f^{pu}N}$. The reason for this unusual expression for the coupling between $P_{0\leftrightarrow 1}$ and light is that the former may be viewed to arise from interference of molecular polarization due to stimulated emission (which depends on $f^{pu}N$), and ground-state bleach, which depends on $(1-f^{pu})N$. (For additional details, including the corresponding double-sided Feynman diagrams, see the SI Sec. II.A.1 and Figure S1.) Ultimately, eq 17 gives a simple interpretation of the three resonances appearing in the vibrational polariton transmission spectrum in the presence of a pump-induced incoherent molecular excited-state population (Figure 4): The PP resonances correspond to transient polaritons formed by the linear coupling of cavity photons to the matter polarization associated with transitions from the molecular ground and excited states. The eigenstate (on the basis of eq 17) associated with each resonance contains the contribution of each type of polarization (cavity photon, $P_{0\leftrightarrow 1}$, and $P_{1\leftrightarrow 2}$) to the corresponding signal in the pump-induced transmission. Importantly, because the output EM field only couples to the cavity photon, the intensity of each resonance of the pump-induced transmission is proportional to the squared absolute value of the photonic component of the corresponding

DOI: 10.1021/acs.jpclett.8b01176
J. Phys. Chem. Lett. 2018, 9, 3766−3771

eigenstate of $h(f^{pu})$. We also note that the mode-coupling matrix provides a connection between the introduced treatment and the classical model (see also ref 50) employed to interpret vibrational-polariton PP transmission spectra in ref 9. This is discussed in detail in the SI Sec. III.

Finally, to gain further insight into the nature of the PP spectrum we compare in Figure 4 the theoretical absolute transmission spectrum of the pump-excited system, $T^{pu}(\omega)$, with the linear spectrum, $T^{0}(\omega)$.

Figure 4 shows that the pump-induced molecular excited-state population leads to a probe response with three resonances, two of which are close to the linear LP frequency and one that is slightly red-shifted from the linear UP. Hence, the reason much larger nonlinear signals are observed for LP relative to UP is that the bare molecule transition $\omega_{1\to2}$ is near-resonant with ω_{LP}, whereas ω_{UP} is far off-resonant with the former. Thus mechanical anharmonicity, which in the delocalized basis leads to polariton−polariton, dark-state−dark-state, and polariton−dark-state interactions,[17,51] has a much weaker effect on UP compared with LP. Given that mechanical anharmonicity also represents the tendency of bonds to break at high energies, we may conjecture that UP states will be more immune to bond dissociation relative to LP. Roughly, this may also be understood from the point of view that the nonlinear signals of UP are much weaker than the LP for the studied system, so the UP behaves more like a harmonic oscillator than the LP. Noting that $\omega_{1\to2} < \omega_{0\to1}$ is a generic property of molecular vibrations, we can conclude that the weaker anharmonic character of the UP quasiparticles relative to LP is likely a general property of vibrational polaritons.

■ ASSOCIATED CONTENT

Supporting Information

The Supporting Information is available free of charge on the ACS Publications website at DOI: 10.1021/acs.jpclett.8b01176.

Complete derivation of Heisenberg−Langevin equations and input−output relations for vibrational polaritons; systematic interpretation of mode-coupling matrix and relationship to classical model of transient response. (PDF)

■ AUTHOR INFORMATION

Corresponding Author

*E-mail: joelyuen@ucsd.edu.

ORCID

Raphael F. Ribeiro: 0000-0002-8605-9665
Wei Xiong: 0000-0002-7702-0187
Jeffrey C. Owrutsky: 0000-0003-3216-7270
Joel Yuen-Zhou: 0000-0002-8701-8793

Notes

The authors declare no competing financial interest.

■ ACKNOWLEDGMENTS

J.Y.-Z and R.F.R acknowledge support from NSF CAREER award CHE:1654732 and generous UCSD startup funds. B.X and W.X. are supported by the AFOSR Young Investigator Program Award, FA9550-17-1-0094, and by the Defense Advanced Research Projects Agency Young Faculty Award program, D15AP000107. B.X acknowledges the Roger Tsien Fellowship from the UCSD Department of Chemistry and Biochemistry. B.S.S., A.D.D., and J.C.O. are supported by the Office of Naval Research through the Institute for Nanoscience at the Naval Research Laboratory. J.Y.-Z acknowledges discussions with Andrea Cavalleri on the various sources of anharmonicities.

■ REFERENCES

(1) Shalabney, A.; George, J.; Hutchison, J.; Pupillo, G.; Genet, C.; Ebbesen, T. W. Coherent Coupling of Molecular Resonators with a Microcavity Mode. *Nat. Commun.* **2015**, *6*, 5981.

(2) Long, J. P.; Simpkins, B. S. Coherent Coupling between a Molecular Vibration and Fabry−Perot Optical Cavity to Give Hybridized States in the Strong Coupling Limit. *ACS Photonics* **2015**, *2*, 130−136.

(3) Simpkins, B. S.; Fears, K. P.; Dressick, W. J.; Spann, B. T.; Dunkelberger, A. D.; Owrutsky, J. C. Spanning Strong to Weak Normal Mode Coupling between Vibrational and Fabry−Pérot Cavity Modes through Tuning of Vibrational Absorption Strength. *ACS Photonics* **2015**, *2*, 1460−1467.

(4) Ahn, W.; Vurgaftman, I.; Dunkelberger, A. D.; Owrutsky, J. C.; Simpkins, B. S. Vibrational Strong Coupling Controlled by Spatial Distribution of Molecules within the Optical Cavity. *ACS Photonics* **2018**, *5*, 158−166.

(5) Vergauwe, R. M. A.; George, J.; Chervy, T.; Hutchison, J. A.; Shalabney, A.; Torbeev, V. Y.; Ebbesen, T. W. Quantum Strong Coupling with Protein Vibrational Modes. *J. Phys. Chem. Lett.* **2016**, *7*, 4159−4164.

(6) Thomas, A.; George, J.; Shalabney, A.; Dryzhakov, M.; Varma, S. J.; Moran, J.; Chervy, T.; Zhong, X.; Devaux, E.; Genet, C.; Hutchison, J. A.; Ebbesen, T. W. Ground-State Chemical Reactivity under Vibrational Coupling to the Vacuum Electromagnetic Field. *Angew. Chem., Int. Ed.* **2016**, *55*, 11462−11466.

(7) Casey, S. R.; Sparks, J. R. Vibrational Strong Coupling of Organometallic Complexes. *J. Phys. Chem. C* **2016**, *120*, 28138−28143.

(8) Crum, V. F.; Casey, S. R.; Sparks, J. R. Photon-Mediated Hybridization of Molecular Vibrational States. *Phys. Chem. Chem. Phys.* **2018**, *20*, 850−857.

(9) Dunkelberger, A. D.; Spann, B. T.; Fears, K. P.; Simpkins, B. S.; Owrutsky, J. C. Modified Relaxation Dynamics and Coherent Energy Exchange in Coupled Vibration-Cavity Polaritons. *Nat. Commun.* **2016**, *7*, 13504.

(10) George, J.; Shalabney, A.; Hutchison, J. A.; Genet, C.; Ebbesen, T. W. Liquid-Phase Vibrational Strong Coupling. *J. Phys. Chem. Lett.* **2015**, *6*, 1027−1031.

(11) Ebbesen, T. W. Hybrid Light−Matter States in a Molecular and Material Science Perspective. *Acc. Chem. Res.* **2016**, *49*, 2403−2412.

(12) Shapiro, M.; Brumer, P. *Principles of the Quantum Control of Molecular Processes*; Wiley-Interscience: Hoboken, NJ, 2003.

(13) Dicke, R. H. Coherence in Spontaneous Radiation Processes. *Phys. Rev.* **1954**, *93*, 99−110.

(14) Hopfield, J. J. Theory of the Contribution of Excitons to the Complex Dielectric Constant of Crystals. *Phys. Rev.* **1958**, *112*, 1555−1567.

(15) Tavis, M.; Cummings, F. W. Exact Solution for an N-Molecule-Radiation-Field Hamiltonian. *Phys. Rev.* **1968**, *170*, 379−384.

(16) Aberra Guebrou, S.; Symonds, C.; Homeyer, E.; Plenet, J. C.; Gartstein, Y. N.; Agranovich, V. M.; Bellessa, J. Coherent Emission from a Disordered Organic Semiconductor Induced by Strong Coupling with Surface Plasmons. *Phys. Rev. Lett.* **2012**, *108*, 066401.

(17) Agranovich, V. M.; Gartstein, Y. N.; Litinskaya, M. Hybrid Resonant Organic−Inorganic Nanostructures for Optoelectronic Applications. *Chem. Rev.* **2011**, *111*, 5179−5214.

(18) Spano, F. C. Optical Microcavities Enhance the Exciton Coherence Length and Eliminate Vibronic Coupling in J-Aggregates. *J. Chem. Phys.* **2015**, *142*, 184707−184720.

(19) Knoester, J. Modeling the Optical Properties of Excitons in Linear and Tubular J-Aggregates. *Int. J. Photoenergy* **2006**, *2006*, 1−10.

(20) Huh, J.; Saikin, S. K.; Brookes, J. C.; Valleau, S.; Fujita, T.; Aspuru-Guzik, A. Atomistic Study of Energy Funneling in the Light-

DOI: 10.1021/acs.jpclett.8b01176
J. Phys. Chem. Lett. 2018, 9, 3766−3771

Harvesting Complex of Green Sulfur Bacteria. *J. Am. Chem. Soc.* **2014**, *136*, 2048−2057.
(21) Virgili, T.; Coles, D.; Adawi, A. M.; Clark, C.; Michetti, P.; Rajendran, S. K.; Brida, D.; Polli, D.; Cerullo, G.; Lidzey, D. G. Ultrafast Polariton Relaxation Dynamics in an Organic Semiconductor Microcavity. *Phys. Rev. B: Condens. Matter Mater. Phys.* **2011**, *83*, 245309.
(22) Hutchison, J. A.; Liscio, A.; Schwartz, T.; Canaguier-Durand, A.; Genet, C.; Palermo, V.; Samorì, P.; Ebbesen, T. W. Tuning the Work-Function Via Strong Coupling. *Adv. Mater.* **2013**, *25*, 2481−2485.
(23) Daskalakis, K. S.; Maier, S. A.; Murray, R.; Kéna-Cohen, S. Nonlinear Interactions in an Organic Polariton Condensate. *Nat. Mater.* **2014**, *13*, 271−278.
(24) Coles, D. M.; Somaschi, N.; Michetti, P.; Clark, C.; Lagoudakis, P. G.; Savvidis, P. G.; Lidzey, D. G. Polariton-Mediated Energy Transfer between Organic Dyes in a Strongly Coupled Optical Microcavity. *Nat. Mater.* **2014**, *13*, 712.
(25) Orgiu, E.; George, J.; Hutchison, J. A.; Devaux, E.; Dayen, J. F.; Doudin, B.; Stellacci, F.; Genet, C.; Schachenmayer, J.; Genes, C.; Pupillo, G.; Samorì, P.; Ebbesen, T. W. Conductivity in Organic Semiconductors Hybridized with the Vacuum Field. *Nat. Mater.* **2015**, *14*, 1123−1129.
(26) Lerario, G.; Fieramosca, A.; Barachati, F.; Ballarini, D.; Daskalakis, K. S.; Dominici, L.; De Giorgi, M.; Maier, S. A.; Gigli, G.; Kéna-Cohen, S.; Sanvitto, D. Room-Temperature Superfluidity in a Polariton Condensate. *Nat. Phys.* **2017**, *13*, 837−841.
(27) Zhong, X.; Chervy, T.; Zhang, L.; Thomas, A.; George, J.; Genet, C.; Hutchison, J. A.; Ebbesen, T. W. Energy Transfer between Spatially Separated Entangled Molecules. *Angew. Chem., Int. Ed.* **2017**, *56*, 9034−9038.
(28) Feist, J.; Garcia-Vidal, F. J. Extraordinary Exciton Conductance Induced by Strong Coupling. *Phys. Rev. Lett.* **2015**, *114*, 196402.
(29) Schachenmayer, J.; Genes, C.; Tignone, E.; Pupillo, G. Cavity-Enhanced Transport of Excitons. *Phys. Rev. Lett.* **2015**, *114*, 196403.
(30) Yuen-Zhou, J.; Saikin, S. K.; Zhu, T.; Onbasli, M. C.; Ross, C. A.; Bulovic, V.; Baldo, M. A. Plexciton Dirac Points and Topological Modes. *Nat. Commun.* **2016**, *7*, 11783.
(31) Herrera, F.; Spano, F. C. Cavity-Controlled Chemistry in Molecular Ensembles. *Phys. Rev. Lett.* **2016**, *116*, 238301.
(32) Kowalewski, M.; Bennett, K.; Mukamel, S. Non-Adiabatic Dynamics of Molecules in Optical Cavities. *J. Chem. Phys.* **2016**, *144*, 054309.
(33) Cortese, E.; Lagoudakis, P. G.; De Liberato, S. Collective Optomechanical Effects in Cavity Quantum Electrodynamics. *Phys. Rev. Lett.* **2017**, *119*, 043604.
(34) Flick, J.; Ruggenthaler, M.; Appel, H.; Rubio, A. Atoms and Molecules in Cavities, from Weak to Strong Coupling in Quantum-Electrodynamics (QED) Chemistry. *Proc. Natl. Acad. Sci. U. S. A.* **2017**, *114*, 3026−3034.
(35) Martínez-Martínez, L. A.; Du, M.; F. Ribeiro, R.; Kéna-Cohen, S.; Yuen-Zhou, J. Polariton-Assisted Singlet Fission in Acene Aggregates. *J. Phys. Chem. Lett.* **2018**, *9*, 1951−1957.
(36) Dunkelberger, A. D.; Davidson, R. B., II; Ahn, W.; Simpkins, B. S.; Owrutsky, J. C. Ultrafast Transmission Modulation and Recovery via Vibrational Strong Coupling. *J. Phys. Chem. A* **2018**, *122*, 965−971.
(37) Mukamel, S. *Principles of Nonlinear Optical Spectroscopy*; Oxford University Press: New York, 1995.
(38) Xiang, B.; Ribeiro, R. F.; Dunkelberger, A. D.; Wang, J.; Li, Y.; Simpkins, B. S.; Owrutsky, J. C.; Yuen-Zhou, J.; Xiong, W. Two-Dimensional Infrared Spectroscopy of Vibrational Polaritons. *Proc. Natl. Acad. Sci. U. S. A.* **2018**, *115*, 4845.
(39) Kavokin, A. V.; Baumberg, J. J.; Malpuech, G.; Laussy, F. P. *Microcavities*; Oxford University Press: Oxford, U.K., 2017.
(40) Khalil, M.; Tokmakoff, A. Signatures of Vibrational Interactions in Coherent Two-Dimensional Infrared Spectroscopy. *Chem. Phys.* **2001**, *266*, 213−230.
(41) Khalil, M.; Demirdöven, N.; Tokmakoff, A. Coherent 2D IR Spectroscopy: Molecular Structure and Dynamics in Solution. *J. Phys. Chem. A* **2003**, *107*, 5258−5279.
(42) Herzberg, G.; Spinks, J. *Molecular Spectra and Molecular Structure: Infrared and Raman Spectra of Polyatomic Molecules*; D. Van Nostrand: Princeton, NJ, 1945.
(43) McCoy, A. B.; Guasco, T. L.; Leavitt, C. M.; Olesen, S. G.; Johnson, M. A. Vibrational Manifestations of Strong Non-Condon Effects in the H3O+·X3 (X = Ar, N2, CH4, H2O) Complexes: A Possible Explanation for the Intensity in the "Association Band" in the Vibrational Spectrum of Water. *Phys. Chem. Chem. Phys.* **2012**, *14*, 7205−7214.
(44) Gardiner, C. W.; Collett, M. J. Input and Output in Damped Quantum Systems: Quantum Stochastic Differential Equations and the Master Equation. *Phys. Rev. A: At., Mol., Opt. Phys.* **1985**, *31*, 3761−3774.
(45) Ciuti, C.; Carusotto, I. Input-Output Theory of Cavities in the Ultrastrong Coupling Regime: The Case of Time-Independent Cavity Parameters. *Phys. Rev. A: At., Mol., Opt. Phys.* **2006**, *74*, 033811−033824.
(46) Portolan, S.; Di Stefano, O.; Savasta, S.; Rossi, F.; Girlanda, R. Nonequilibrium Langevin Approach to Quantum Optics in Semiconductor Microcavities. *Phys. Rev. B: Condens. Matter Mater. Phys.* **2008**, *77*, 035433−035450.
(47) Li, H.; Piryatinski, A.; Jerke, J.; Kandada, A. R. S.; Silva, C.; Bittner, E. R. Probing Dynamical Symmetry Breaking Using Quantum-Entangled Photons. *Quantum Sci. Technol.* **2018**, *3*, 015003−015017.
(48) Yuen-Zhou, J.; Krich, J.; Aspuru-Guzik, A.; Kassal, I.; Johnson, A. *Ultrafast Spectroscopy: Quantum Information and Wavepackets*; IOP Publishing, 2014.
(49) Mukamel, S.; Nagata, Y. Quantum Field, Interference, and Entanglement Effects in Nonlinear Optical Spectroscopy. *Procedia Chem.* **2011**, *3*, 132−151.
(50) Fofang, N. T.; Grady, N. K.; Fan, Z.; Govorov, A. O.; Halas, N. J. Plexciton dynamics: exciton− plasmon coupling in a J-aggregate−Au nanoshell complex provides a mechanism for nonlinearity. *Nano Lett.* **2011**, *11*, 1556−1560.
(51) Carusotto, I.; Ciuti, C. Quantum Fluids of Light. *Rev. Mod. Phys.* **2013**, *85*, 299−366.

DOI: 10.1021/acs.jpclett.8b01176
J. Phys. Chem. Lett. 2018, 9, 3766−3771